arXiv:1703.03281v1 [cond-mat.soft] 9 Mar 2017

Nanoscale Seebeck effect of thermally powered active Janus colloids

Aboubakry Ly[1], Arghya Majee[2,3], Alois Würger[1]
[1] *Laboratoire Ondes et Matière d'Aquitaine, Université de Bordeaux & CNRS, 33405 Talence, France*
[2] *Max-Planck-Institut für Intelligente Systeme, 70569 Stuttgart, Germany and*
[3] *IV. Institut für Theoretische Physik, Universität Stuttgart, 70569 Stuttgart, Germany*

We theoretically study the Seebeck effect in the vicinity of a heated metal nanostructure, such as the gold cap of an active Janus colloid in an electrolyte. The thermocharge varies with the surface temperature, thus modulating the diffuse layer of an insulating surface, and inducing polarization charges on an electric conductor. The isopotential boundary condition on a metal surface, results in a reduction of the slip velcoity. Our results agree with recently observed specific-ion effects for Janus colloids in different electrolyte solutions. Comparing the thermal, hydrodynamic, and ion diffusion time scales, we expect a rich transient behavior at the onset of thermally powered swimming, ranging well beyond microseconds.

Laser-heated metal nanostructures provide versatile and easy-to-use local heat sources, with applications ranging from photothermal imaging [1] and cancer therapy [2], to thermally powered artificial microswimmers [3]. The latter rely on the conversion of heat to motion; experimental realizations include metal-capped Janus particles driven by surface forces [3, 4], and interface floaters that are advected by their self-generated Marangoni flow [5, 6]. Force-free localization and steering have been achieved by temporal [7] or spatial [8] modulation of the laser power. There is strong evidence that clustering and collective behavior of active colloids are generic properties that are determined by the particle geometry [9] and hydrodynamic interactions [10].

In contrast, in recent years a variety of heat-flow induced swimming mechanisms have been pointed out, such as diffusiophoresis due to local phase separation in a near-critical mixture [4] or thermo-osmotic flow towards a hot spot in a capillary [11]. These experiments also revealed strong dependencies on material properties: Thus the opposite swimming direction was observed upon rendering the particle's active cap hydrophilic instead of hydrophobic [4], or upon adding a non-ionic surfactant to the solvent [3]. Similarly, copolymer coating of a glass surface increased the thermo-osmotic velocity by one order of magnitude [11]. Catalytic swimmers are sensitive to material properties of their surface [12] or of nearby solid boundaries [13].

A particularly intriguing specific-ion effect was reported very recently for silica colloids carrying a gold cap: their swimming velocity in a 10 mM NaCl solution changed significantly when replacing the cation with lithium, or the anion with hydroxide [14]. These findings indicate that self-propulsion depends on the electrolyte Seebeck effect [15], confirming previous observations on passive particles in an external temperature gradient [16–18]. Recently an enhanced Seebeck-induced flow was predicted in confined geometries [19]. At present it is not clear, however, how the slip velocity v_s changes at an active surface with self-generated Seebeck field, nor whether v_s takes a finite value, or zero, at a metal surface.

In this Letter we study how the thermoelectric self-propulsion of hot Janus particles depends on surface properties and in particular, how it is modified by the electric conductivity of the metal cap. This latter question amounts to determining the electroosmotic coefficient at a conducting or isopotential surface; besides the specific problem of thermally powered microswimmers, it is relevant for electrophoresis of metal particles and, more generally, for hot metal structures in contact with an electrolyte solution.

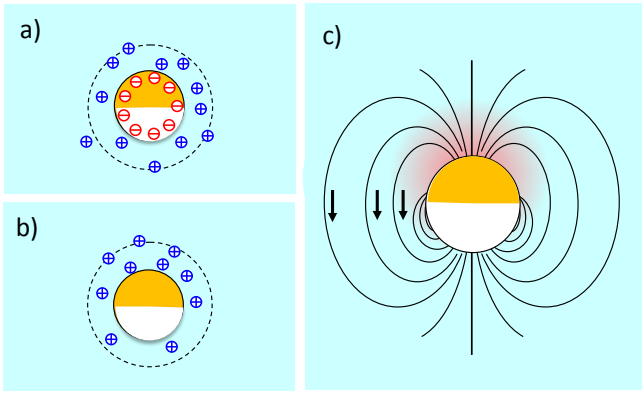

FIG. 1: Thermoelectric driving of a heated Janus particle. a) The electric double layer of a charged particle. Its thickness, indicated by the dashed line, is not at scale, in real systems the Debye length λ is about hundred times smaller than the particle radius ($a \sim 1\mu$m). b) Thermocharge accumulated by the electrolyte Seebeck effect ($S < 0$); the resulting (positive or negative) thermocharge density is larger at the hot metal cap; for an excess temperature of a few Kelvin one has a net charge of about $Q \sim 100e$ [21]. c) Thermo-electric field lines in the vicinity of the particle (for clarity we have discarded the monopole contribution $Q/4\pi\varepsilon r^2$). The parallel component $E_{||}$ is finite at the insulating surface (lower hemisphere), but vanishes at the metal cap.

Electrolyte Seebeck effect. In an electrolyte solution with non-uniform temperature, positive and negative salt ions migrate along the gradient at a velocity $-\mu_\pm h_\pm \nabla T/T$ which is given by the ion-specific mobility $\mu_\pm$ and enthalpy of transport $h_\pm$ [20]. In the steady state,

opposite thermocharges accumulate at the cold and hot boundaries of the liquid phase, giving rise to a macroscopic thermoelectric field

$$\mathbf{E} = S\nabla T \qquad \text{(far-field)}, \tag{1}$$

where the Seebeck coefficient $S = (h_+ - h_-)/2eT$ is of the order of 100 μV/K and may take either sign.

Fig. 1 illustrates the Seebeck effect in the vicinity of a laser-heated Janus colloid. Since the particle surface constitutes the hot boundary of the liquid phase, the corresponding thermocharge (b) is superposed on the particle's counterion cloud (a). Well beyond the Debye screening length λ, one finds the long-range thermoelectric field (1). An excess temperature of a few Kelvin, results in a thermocharge of about 100 elementary charges, and in a field of the order of kV/m [21]. In Fig. 1c we have substracted the monopole contribution $\propto r^{-2}$ which corresponds to the isotropic part of the temperature gradient. Note that the thermocharge is not screened; its counterions are at the cell boundary. The corresponding thermopotential $\varphi(\mathbf{r}) = -S[T(\mathbf{r}) - T_0]$ comprises a monopole term that decays with the inverse distance [21].

The principle of self-generated thermo-electrophoresis follows from Fig. 1c: The parallel component $E_{||}$ of the Seebeck field acts on the particle's double layer, inducing an electro-osmotic flow which in turn results in an opposite motion of the particle [22]. In the example shown here, the negative ζ-potential and Seebeck coefficient S imply a positive diffuse layer $\rho > 0$, an upward slip velocity and thus an downward motion of the particle.

Non-equilibrium double layer. A quantitative description for the electrostatic properties is obtained from Poisson-Boltzmann theory, albeit with an unusual outer boundary condition: Well beyond the double layer, the electric field is given by (1), contrary to the vanishing far-field of an equilibrium double layer. The boundary conditions at the particle surface depend on its electrical conductivity: At the insulating hemisphere we impose the surface charge σ_0; and constant ζ-potential at the metal cap.

We are mainly interested in the electric field close to the particle surface, which has, however, to be matched to the far-field (1). To achieve this, we assume (i) that the Debye length is much smaller than the particle radius, $\lambda \ll a$, and (ii) that the thermocharge is much smaller than the particle's surface charge. These assumptions are well justified for micron-sized colloids, and constitute the widely used boundary-layer approximation [22]: It implies that the double-layer is in equilibrium perpendicular to the particle surface, the non-equilibrium nature arises along the particle surface.

We first consider an insulating surface, such as the lower hemisphere of the particle in Fig. 1c. The usual electrostatic boundary condition relate the normal field component to the surface charge density σ_0 [23],

$$E_\perp|_{\text{ins}} = -\sigma_0/\varepsilon. \tag{2}$$

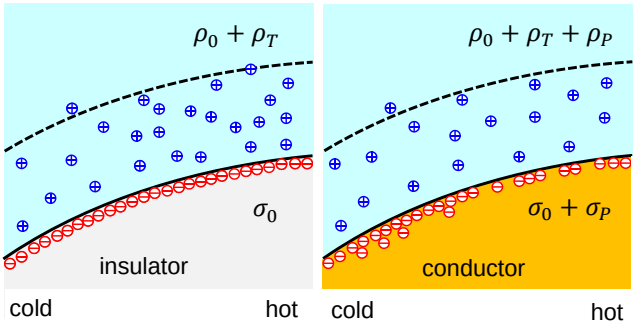

FIG. 2: Electric double-layer including the thermocharge (temperature increases from left to right). At an insulating surface, the surface charge density σ_0 is not affected by the Seebeck effect, whereas the diffuse layer comprises the non-uniform thermocharge density ρ_T. At a conducting surface (right panel), the condition of a constant surface potential requires a polarization charge σ_P; the corresponding counterions exactly cancel the non-uniform thermocharge, such that the diffuse layer contains a constant charge density. For typical Seebeck coefficients, the charge modulation ρ_T/ρ_0 (or σ_P/σ_0) is of the order of the relative temperature change $\Delta T/T$.

With the above assumptions, it is straightforward to modify the known solution of (2) in such a way that it satisfies the far-field condition (1). In addition to the counterion charge density ρ_0, the diffuse layer contains the thermocharge [25],

$$\rho_T = \frac{\varepsilon S \nabla_\perp T}{\lambda} e^{-z/\lambda} \frac{(1-g^2)(1+\hat{g}^2)}{(1-\hat{g}^2)^2} \tag{3}$$

where $\hat{g} = e^{-z/\lambda} g$ and where the parameter $g = (1 + \ell^2/\lambda^2)^{1/2} - \ell/\lambda$ depends on the ratio of the Gouy-Chapman and Debye lengths ℓ and λ [23]. Because of the non-uniform temperature along the surface, $\nabla_\perp T$ slowly varies along the surface, and so does the thermocharge density ρ_T, as illustrated in Fig. 2. More interestingly, the thermocharge results in a parallel thermoelectric field

$$E_{||}^{\text{ins}} = S\nabla_{||} T, \tag{4}$$

which corresponds to the far-field expression (1) and decays slowly at the scale of the particle size.

Now we turn to the conducting gold cap of the upper hemisphere in Fig. 1c. Because of its high electric and thermal conductivities, this metal layer may considerably modify the thermoelectric properties and the induced boundary flow. A sufficiently thick gold cap of about hundred nanomters, forms an isotherm and thus has zero slip velocity [24]. A thin cap, of ten nanometers or less, does not alter the temperature gradient but forms an isopotential surface; the electrostatic boundary

conditions impose a vanishing parallel electric field [23]

$$E_{||}|_{\rm cond} = 0. \tag{5}$$

This requires a non-uniform surface charge density σ of the metal layer, as illustrated in the rigth panel of Fig. 2. The mobile electrons in the metal surface move until their polarization charge density σ_P cancels the parallel component (4) of the thermoelectric field. It turns out that the corresponding polarization of the double layer, ρ_P, cancels the thermocharge to leading order in λ/a. The resulting parallel field in the vicinity of the particle then reads

$$E_{||}^{\rm cond}(z) = \left(1 - \frac{1-g^2}{1-\hat{g}^2} e^{-z/\lambda}\right) S\nabla_{||}T. \tag{6}$$

As illustrated in Fig. 1c, it vanishes at the surface, whereas well beyond the screening layer, it tends towards the macroscopic Seebeck field (1).

Slip velocity. The parallel electric field exerts a force on the particle's counter ions which in turn drag the solvent and thus induce a slip velocity v_s. At an insulating surface, this field (4) decreases slowly on the scale of the particle radius; thus we may take its value at the surface and find

$$v_s^{\rm ins} = \frac{\varepsilon\zeta}{\eta} S\nabla_{||}T, \tag{7}$$

with the viscosity η and permittivity ε of water. A more complex situation occurs at a conducting surface, since the parallel thermoelectric field vanishes at the surface and then strongly increases on the scale of the screening length. Integrating the Helmholtz-Smoluchowski expression $v_s = \frac{1}{\eta}\int_0^\infty dz z\rho(z)E_{\|}(z)$ with the varying field (6), we have

$$v_s^{\rm cond} = \left(1 - \frac{k_BT}{e\zeta}\tanh\frac{e\zeta}{4k_BT}\right)\frac{\varepsilon\zeta}{\eta} S\nabla_{||}T. \tag{8}$$

Thus the slip velocity at a conducting surface is only slightly smaller than at an insulator. In the weak-coupling range $e|\zeta| < k_BT$, the factor in parenthesis takes the value $\frac{3}{4}$; it slightly increases at highly charged surfaces.

At first sight, one could have expected that the thermoelectric slip velocity along a conducting surface vanishes because of the zero field boundary condition $E_{||}^{\rm cond}(0) = 0$. Our analysis shows that this is not the case and that the slip velocity is merely reduced by a numerical factor $\frac{3}{4}$.

Granular gold surface. The above discussion assumes a continuous gold cap, which does not always correspond to the actual experimental situation. For example, the cap of the particles used in Ref. [14] consists of a dense coverage of nano-sized gold grains, visible in scanning electron microscopy images [26] and illustrated in Fig. 3.

These grains do not connect to a continuous gold structure. Each of them forms an equipotential surface, implying that the parallel field vanishes within one screening layer, as in Eq. (6). Yet there is a potential jump between nearby grains; their cold and hot boundaries carry polarization charges which result in a strong electric field in the spacing, as illustrated in Fig. 3. As a consequence, the picture developed for micron-size conducting surfaces remains correct at the nanoscale. Because of the surface roughness one may expect a somewhat smaller slip velocity than at a homogeneous cap.

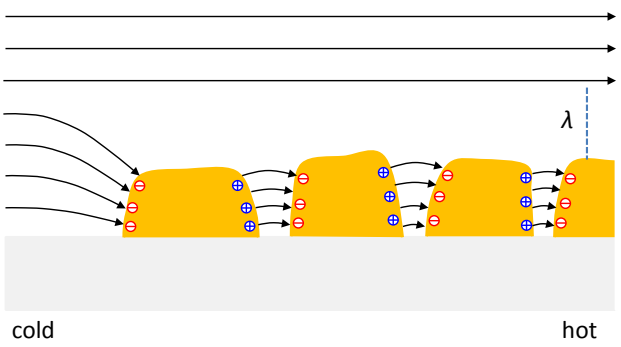

FIG. 3: Parallel component $E_{||}$ of the thermoelectric field in the vicinity of a granular gold cap ($S > 0$). Each metal grain forms an equipotential surface and carries opposite polarization charges σ_P at its cold and hot sides. Like on the continuous cap in Fig. 1c, $E_{||}$ vanishes in a layer of about one screening length. On the insulating surface at the left, the field is given by (4).

A recent experiment reported thermo-electric driving of hot silica particles with a granular gold cap [14]. Probing the particle's self-propulsion velocity in 10 mM solutions of NaCl, LiCl and NaOH, revealed a strong salt-specific effect, which agrees qualitatively with the Seebeck coefficients of these electrolytes, $S_{\rm NaCl} > S_{\rm LiCl} > S_{\rm NaOH}$. When comparing to experimental findings, one has to add to v_s the thermo-osmotic and related contributions, subsumed in $v_s^{\rm osm}$, which are of comparable magnitude but independent of the ion species [18].

Contrary to what was observed for passive polystyrene beads in an external temperature gradient [18], the negative Seebeck effect of NaOH does not result in a change of sign of the self-propulsion velocity of an active particle [14]. This could be related to the reduction of the slip velocity at the gold cap (8): Because of the factor $\frac{3}{4}$, the negative thermoelectric driving in NaOH solution would not be sufficient to the overcome the thermoosmotic velocity. As another possible explanation, we mention the strong increase of $v_s^{\rm osm}$ with temperature, whereas the thermoelectric contribution was found to be rather constant [18]. Finally, it has been shown that an additional thermally induced electric field may arise from the alignement of water molecules on the temperature gradient [27, 28].

Transient and memory effects. So far we have considered the steady-state Seebeck effect. The transient behavior after switching on the heat source is readily ob-

tained from the advection-diffusion equation for the ions with Gauss' law $\nabla \cdot E = -\rho/\varepsilon$. Thus we find

$$\rho_T(t) = \rho_T(\infty)(1 - e^{-t/\tau}), \tag{9}$$

where the characteristic time scale expresses the time of ion diffusion over the screening length,

$$\tau_{\rm ion} = \frac{\lambda^2}{2D}. \tag{10}$$

With typical values $D \sim 10^{-9}$ m^2/s and $\lambda \sim 50$ nm, one finds $\tau \sim \mu$s. Thus building up the Seebeck field requires a few microsceconds, and the same time-dependence occurs for the slip velocity. Indeed, the thermal and hydrodynamic time scales, $\tau_{\rm th} = \lambda^2/\alpha$ and $\tau_{\rm hy} = \lambda^2/\nu$, are by several orders of magnitude shorter, since both heat diffusivity ($\alpha \sim 10^{-7}$ m^2/s) and kinematic viscosity ($\nu \sim 10^{-6}$ m^2/s), by far exceed ion diffusivity. It should be noted that $\tau_{\rm hy}$ is much shorter than the hydrodynamic memory of Brownian motion, $\tau'_{\rm hy} = a^2/\nu$ [29]; this is due to the fact that in the latter case, the hydrodynamic stress decays over the particle size a, whereas for phoretic and active particles, the relevant stress is confined within the interaction length λ [30].

As a consequence, we expect a rather intricate behavior of the particle motion during the the first milliseconds,

$$v_s(t) = v_s^{\rm el}(1 - e^{-t/\tau_{\rm ion}}) + v_s^{\rm osm}(1 - e^{-t/\tau_{\rm th}}). \tag{11}$$

The thermo-osmotic slip velocity $v_s^{\rm osm}$ sets in on the heat-diffusion time scale $\tau_{\rm th} \sim 10$ nanoseconds. The Seebeck effect requires ion diffusion which occurs on the time scale $\tau_{\rm ion}$ that may attain a microsecond. Since in many instances, the thermoelectric slip velocity $v_s^{\rm el}$ is stronger and carries the opposite sign [17, 18], the onset of the Seebeck effect could even result in a reversal of the direction of motion.

The above discussion applies to the double-layer at the conducting hemisphere, where the local temperature gradient is determined by absorption of laser light by the gold coating. At the insulating hemisphere, however, building up the stationary temperature profile requires heat diffusion over a distance comparable to the particle radius. Thus the thermal time scale, $\tau_{\rm th}^{\rm ins} = a^2/\alpha$, is of the order of ten microseconds, and exceeds the duration of the transients within the double layer.

In summary, we find that the self-propulsion of hot Janus particles strongly depends on the electrolyte Seebeck effect, involving both surface material and ion-specific properties, in qualitative agreement with a recent experiment [14]. On insulating materials, the diffuse layer comprises a thermocharge ρ_T which is proportional to the surface excess temperature. On a conductor, however, the parallel temperature gradient induces a polarization charge, the counterions of which cancel the non-uniform part of ρ_T. In other words, the parallel Seebeck field on insulating surfaces is generated by mobile ions in the diffuse layer, whereas on conducting materials it arises from the polarization of the electron gas. As a most striking result, the thermoelectric field (6) vanishes at the conducting surface, yet strongly increases through the Debye layer. The resulting slip velocity corresponds to about $\frac{3}{4}$ of the value on an insulator. Because of the slow diffusion of ions, as compared to diffusion of heat and momentum, the thermo-electric slip velocity sets in on a timescale of microseconds, giving rise to an intricate transient behavior upon switching on the heating.

AL and AW acknowledge support by Agence Nationale de la Recherche through contract ANR-13-IS04-0003.

[1] D. Boyer, P. Tamarat, A. Maali, B. Lounis, and M. Orrit, Science **297**, 1160 (2002).

[2] G. Baffou and R. Quidant, Laser Photonics Rev. 7, 171 (2013).

[3] H.-R. Jiang, N. Yoshinaga, M. Sano, Phys. Rev. Lett. **105**, 268302 (2010).

[4] I. Buttinoni, G. Volpe, F. Kümmel, G. Volpe, and C. Bechinger, J. Phys.: Cond. Mat. **24**, 284129 (2012).

[5] A. Girot, N. Danné, A. Würger, T. Bickel, F. Ren, J. C. Loudet, and B. Pouligny, Langmuir **32**, 2687 (2016).

[6] A. Würger, J. Fluid Mech. **752**, 589 (2014).

[7] A. P. Bregulla, H. Yang, and F. Cichos, ACS Nano **8**, 6542 (2014).

[8] C. Lozano, B. ten Hagen, H. Löwen, and C. Bechinger, Nat. Commun. **7**, 12828 (2016).

[9] I. Buttinoni, J. Bialke, F. Kümmel, H. Löwen, C. Bechinger, and T. Speck, Phys. Rev. Lett. **110**, 238301 (2013).

[10] A. Zöttl1 and H. Stark, Phys. Rev. Lett. **112**, 118101 (2014).

[11] A. P. Bregulla, A. Würger, K. Günther, M. Mertig, and F. Cichos, Phys. Rev. Lett. **116**, 188303 (2016).

[12] S. Ebbens, D. A. Gregory, G. Dunderdale, J. R. Howse, Y. Ibrahim, T. B. Liverpool, and R. Golestanian, EPL, **106**, 58003 (2014).

[13] W. E. Uspal, M. N. Popescu, S. Dietrich, and M. Tasinkevych, Phys. Rev. Lett. **117**, 048002 (2016).

[14] S. Simoncelli, J. Summer, S. Nedev, P. Kühler, and J. Feldmann, Small **29**, 2854 (2016).

[15] A. Würger, Rep. Prog. Phys. **73,** 126601 (2010).

[16] S. A. Putnam and D. G. Cahill, Langmuir **21**, 5317 (2005).

[17] D. Vigolo, S. Buzzaccaro, and R. Piazza, Langmuir **26**, 7792 (2010).

[18] K. A. Eslahian, A. Majee, M. Maskos, A. Würger, Soft Matter **10**, 1931 (2014).

[19] M. Dietzel and S. Hardt, Phys. Rev. Lett,**116**, 225901 (2016).

[20] S. R. de Groot and P. Mazur, *Non-equilibrium Thermodynamics*, North-Holland Publishing, Amsterdam, 1962.

[21] A. Majee and A. Würger, Phys. Rev. Lett. **108**, 11803 (2012).

[22] J. L. Anderson, Annu. Rev. Fluid Mech. **21**, 61 (1989).
[23] D. Andelman, In *Soft Condensed Matter Physics in Molecular and cell Biology,* Poon, W., Andelman, D. (eds.), Scottish Graduate Series (Taylor and Francis 2006).
[24] T. Bickel, A. Majee, and A. Würger, Phys. Rev. E **88**, 012301 (2013).
[25] See appendix C.
[26] S. Nedev, S. Carretero-Palacios, P. Kühler, T. Lohmüller, A. S. Urban, L. J. E. Anderson, and J. Feldmann, ACS Photonics **2,** 491 (2015).
[27] J. Armstrong, C. D. Daub, and F. Bresme, J. Chem. Phys. **143**, 036101 (2015).
[28] D. Frenkel, J. Phys. Chem. B **120**, 5987 (2016).
[29] T. Franosch, M. Grimm, M. Belushkin, F. M. Mor, G. Foffi, L. Forró, and Sylvia Jeney, Nature **478**, 85 (2011).
[30] S. Fayolle, T. Bickel, and A. Würger, Phys. Rev. E **77**, 041404 (2008).

Appendix

Here we present the detailed calculation for the properties of the electric double-layer in the presence of a temperature gradient, and in particular evaluate the effect of a conducting surface on the Seebeck field in the vicinity of the particle and the resulting electrophoretic mobility.

Sections A and B give the essential formulae of the 1D Poisson-Poisson-Boltzmann solution for a charged surface and for the bulk electrolyte Seebeck effect. In Sections C and D we show how the electric double-layer is affected by the Seebeck effect, and we derive the double-layer properties for insulating and conducting surfaces in a temperature gradient.

Appendix A: Poisson-Boltzmann theory

In mean-field theory, the electrostatic potential φ of a charged surface in contact with an electrolyte solution, satisfies the Poisson-Boltzmann equation

$$\nabla^2\varphi = \frac{k_BT}{e\lambda^2}\sinh\frac{e\varphi}{k_BT}. \tag{A1}$$

If the particle radius is much larger than the Debye screening length, the curvature of the surface can be neglected. Then the Laplace operator reduces to the second derivative with respect to the vertical coordinate z, and the potential is the 1D solution [23]

$$\varphi_0(z) = -\frac{2k_BT}{e}\ln\frac{1+ge^{-z/\lambda}}{1-ge^{-z/\lambda}}, \tag{A2}$$

where the parameter

$$g = \sqrt{1+\ell^2/\lambda^2} - \ell/\lambda \tag{A3}$$

is given by the ratio of the Gouy-Chapman length ℓ and the Debye length λ,

$$\ell = \frac{e}{2\pi\ell_B|\sigma_0|}, \qquad \lambda = \frac{1}{\sqrt{8\pi\ell_B n_0}}. \tag{A4}$$

Here we use the Bjerrum length ℓ_B, the surface charge densitiy σ_0, and the salinity n_0. We assume a negative surface charge $\sigma_0 < 0$.

The electric field is perpendicular to the surface and reads

$$E = -\frac{d\varphi_0}{dz} = \frac{4k_BT}{e\lambda}\frac{\hat g}{1-\hat g^2} \tag{A5}$$

with the shorthand notation

$$\hat g = ge^{-z/\lambda}.$$

The charge density in the diffuse layer reads

$$\rho_0 = \varepsilon\frac{dE}{dz} = \frac{4k_BT}{e\lambda^2}\hat g\frac{1+\hat g^2}{1-\hat g^2}. \tag{A6}$$

With the definition of g one readily verifies the relation between the electric field at the solid boundary B and the surface charge,

$$E|_B = -\frac{\sigma_0}{\varepsilon}.$$

For further use we rewrite the electric field as

$$E = \frac{4k_BT}{e\lambda}\frac{\hat g}{1-\hat g^2} = -\frac{\sigma_0}{\varepsilon}e^{-z/\lambda}\frac{1-g^2}{1-\hat g^2}. \tag{A7}$$

Appendix B: Seebeck effect at an uncharged boundary

Here we review the electrolyte Seebeck effect and the related thermocharge close to an uncharged insulating surface.

1. Far-field

Consider a monovalent electrolyte solution with concentrations n_+ and n_- for respectively positive and negative ions, subject to a temperature gradient. Then the ion currents read

$$\mathbf{J}_\pm = -D_\pm\left(\nabla n_\pm + 2n_\pm\frac{h_\pm}{k_BT}\frac{\nabla T}{T} \mp n_\pm\frac{e\mathbf{E}}{k_BT}\right), \tag{B1}$$

where the terms in parentheses account for gradient diffuson, thermal diffusion, and electrophoresis in the self-generated electric field. In the steady state the currents vanish. Imposing charge neutrality in the bulk we find the macroscopic thermoelectric field

$$\mathbf{E} = S\nabla T, \tag{B2}$$

with the Seebeck coefficient

$$S = \frac{h_+ - h_-}{2eT}.$$

The corresponding thermopotential reads

$$\varphi_T(\mathbf{r}) = -S(T(\mathbf{r}) - T_0),$$

where $T(\mathbf{r}) - T_0$ is the excess temperature due to heating.

2. Thermocharge and near-field

Usual electrostatic boundary conditions require that the electric field normal to a solid surface B vanishes,

$$E_\perp|_B = 0.$$

At the hot and cold boundaries, the macroscopic Seebeck field is screened by a layer of positive or negative ions. Thus in the vicinity of the boundaries, the above expressions for φ_T and $\mathbf{E}$ have to be modified.

The thermocharge density ρ_T satisfies Gauss' law

$$\partial_z E_\perp|_B = -\rho_T/\varepsilon.$$

In the absence of other surface charges, one readily finds

$$\rho_T(z) = \frac{\varepsilon S \nabla_\perp T}{\lambda} e^{-z/\lambda}, \tag{B3}$$

where $\nabla T_\perp$ is the normal component of the temperature gradient. Here and in the following we assume that the temperature gradient hardly varies on the scale of the screening length, and thus may be taken as a constant when calculating $\partial_z E_\perp$. Then we obtain the charge per unit area by integrating the exponential factor,

$$\int_0^\infty dz \rho_T = \varepsilon S \nabla_\perp T. \tag{B4}$$

By the same token, Gauss' law is readily integrated, and the normal component of the electric field reads

$$E_\perp = S\nabla_\perp T(1 - e^{-z/\lambda}). \tag{B5}$$

In the case of an insulating surface, the parallel component is not affected,

$$E_{||} = S\nabla_{||} T.$$

Integrating once more we find the thermopotential

$$\varphi_T = -S(T - T_0) - \lambda e^{-z/\lambda} S \nabla_\perp T|_B.$$

The first term is present throughout a macroscopic cell and is proportional to the local excess temperature. The second term is finite only within the screening layer and hardly modifies the thermopotential.

Appendix C: Seebeck effect at an insulating charged surface

Now we consider the case where the boundary carries a surface charge σ_0 which is screened by a diffuse layer of thickness λ and charge concentration ρ_0. Colloidal surfaces are usually strongly charged, such that the Debye-Hückel approximation does not apply. Then the thermocharge concentration does not follow exponential screening like in (B3) but shows the more complex dependence of the Poisson-Boltzmann solution.

We first consider an insulating surface with non-uniform temperature. In general the thermal gradient has normal and parallel components, $\nabla_\perp T$ and $\nabla_{||} T$, resulting in corresponding components of the Seebeck field. The usual electrostatic boundary condition relate the normal field component to the surface charge density σ_0 [23],

$$E_\perp|_{\rm ins} = -\sigma_0/\varepsilon. \tag{C1}$$

In other words, the normal Seebeck component at the surface vanishes. Like in (B5), it is screened by the thermocharge ρ_T.

1. Thermocharge ρ_T

Since the thermocharge density ρ_T is about hundred times smaller than that of the double layer ρ_0, it does not modify the profile of the diffuse layer. The thermocharge per unit area is given by Eq. (B4). Then the overall charge density in the diffuse layer is obtained as

$$\rho = \rho_0 + \rho_T = \rho_0 + \frac{d\rho_0}{d\sigma_0} \varepsilon S \nabla_\perp T.$$

The last term is readily calculated from (A2) and (A4), resulting in

$$\rho_T = \frac{\varepsilon S \nabla_\perp T}{\lambda} e^{-z/\lambda} \frac{(1-g^2)(1+\hat{g}^2)}{(1-\hat{g}^2)^2}. \tag{C2}$$

In vertical direction z, the thermocharge decays exponentially on the scale of the screening length λ.

2. Thermoelectric field

From Gauss's law

$$\partial_z E_\perp = -(\rho_0 + \rho_T)/\varepsilon - \delta(z)\sigma_0/\varepsilon$$

we find the normal component of the electric field,

$$E_\perp = S\nabla_\perp T - \left(S\nabla_\perp T + \frac{\sigma_0}{\varepsilon}\right) e^{-z/\lambda} \frac{1-g^2}{1-\hat{g}^2}. \tag{C3}$$

At large distances well beyond the screening layer, the second term vanishes and one recovers the far-field (B2), whereas at the surface ($z = 0$) the field satisfies (C1). $E_\perp$ varies more slowly along the particle surface, on the scale of the particle size, due to the non-uniform normal component of the temperature gradient $\nabla_\perp T$.

In addition to the perpendicular gradient that appears in (C2), the temperature field of the heated cap varies along the particle surface; the component $\nabla_{||} T$ gives rise to the parallel Seebeck field

$$E_{||}^{\rm ins} = S\nabla_{||} T, \tag{C4}$$

which matches the far-field. Since $\nabla_{||} T$ varies on the scale of the particle radius, the parallel electric field is constant within the screening length.

Appendix D: Seebeck effect at a conducting charged surface

Now we turn to the conducting gold cap of the upper hemisphere in Fig. 1c. The electrostatic boundary conditions impose a constant potential [23], and a vanishing parallel electric field,

$$\varphi|_{\rm cond} = {\rm const}, \quad E_{||}|_{\rm cond} = 0. \tag{D1}$$

Together with the far-field condition (B2), Eq. (D1) requires a non-uniform surface charge density σ of the metal layer.

1. Polarization charge σ_P

The mobile electrons in the metal surface move until their polarization charge density σ_P cancels the parallel component of the thermoelectric field (B2) at the surface. In order to calculate the polarization charge, we consider the Poisson-Boltzmann potential of a slowly varying surface charge $\sigma = \sigma_0 + \sigma_P$, linearize in terms of σ_P, and impose that the overall electric field vanishes at the surface. Thus we find

$$\sigma_P = -\varepsilon S \left(\nabla_\perp T - \langle \nabla_\perp T \rangle \right), \tag{D2}$$

where $\langle ... \rangle$ indicates the surface average. This constant term simply accounts for the fact that the Seebeck effect merely polarizes gold structure, without changing its overall charge.

Since the diffuse layer screens the local surface charge density, σ_P induces a corresponding change of the mobile charge density, ρ_P. It turns out that ρ_P cancels the anisotropic part of the thermocharge ρ_T to leading order in λ/a,

$$\rho = \rho_0 + \rho_T + \rho_P = \rho_0 + \langle \rho_T \rangle .$$

In other words, the mobile charge density in the diffuse layer is roughly constant along the metal surface.

2. Thermoelectric field

The double-layer charge consisting of ρ and σ as discussed above, results in Gauss's law

$$\partial_z E_\perp = -\frac{\rho_0 + \langle \rho_T \rangle}{\varepsilon} - \delta(z) \frac{\sigma_0 + \sigma_P}{\varepsilon}.$$

Using the relation between ρ_0 and σ_0, we find the normal component of the electric field,

$$E_\perp = S \nabla_\perp T - \left(S \langle \nabla_\perp T \rangle + \frac{\sigma_0}{\varepsilon} \right) e^{-z/\lambda} \frac{1 - g^2}{1 - \hat{g}^2}. \tag{D3}$$

At the surface we have $E_\perp|_B = -(\sigma_0 + \sigma_P)/\varepsilon$, whereas at large distances $E_\perp$ corresponds to the far-field expression (B2).

The resulting parallel field in the vicinity of the particle reads

$$E_{||}^{\mathrm{cond}}(z) = \left(1 - \frac{1 - g^2}{1 - \hat{g}^2} e^{-z/\lambda} \right) S \nabla_{||} T. \tag{D4}$$

Note that this expression vanishes at the surface, $E_{||}^{\mathrm{cond}}(0) = 0$, whereas well beyond the screening layer, it tends towards the macroscopic Seebeck field (B2).